Mechanics of Soft Materials (2020) 2: 1
https://doi.org/10.1007/s42558-019-0016-y

ORIGINAL PAPER

The two Poisson's ratios in annulus fibrosus: relation with the osmo-inelastic features

Amil Derrouiche[1] · Anouar Karoui[2] · Fahmi Zaïri[1] · Jewan Ismail[1] · Zhengwei Qu[1] · Makram Chaabane[2] · Fahed Zaïri[3]

Received: 28 November 2019 / Accepted: 19 December 2019 / Published online: 31 January 2020

Abstract
The annulus fibrosus of the intervertebral disc is a highly complex layered structure in which the inelastic features of the tangled extracellular matrix interact with the surrounding physiological fluid by osmotic effect. In this in vitro study, the time-dependent transversal behavior in the two planes (fibers and lamellae planes) of multi-lamellae annulus tissues is reported by means of an accurate optical strain measuring technique based upon digital image correlation. Fresh annulus specimens of square cross section, extracted from bovine cervical discs, are tested under quasi-static (cyclic uniaxial stretching) and relaxation (interrupted stretching) loading with variation in osmolarity and strain rate conditions. Significant osmotic and strain rate effects are found on the elastic stiffness and the apparent Poisson's ratios ($p < 0.05$, ANOVA). Under quasi-static loading, the apparent Poisson's ratio is found higher than 0.5 in fibers plane and negative (i.e., auxetic) in lamellae plane. This material property evolves progressively towards classical bounds with relaxation time, i.e., between 0 and 0.5. The strong dependence of the auxetic behavior on time and chemical environment provides valuable insights about internal fluid exchanges. An interpretation of the osmo-inelastic mechanisms is proposed in which mechanical-based and chemical-based fluid flow interact until chemo-mechanical equilibrium. The new information allows a better understanding of the disc functionality and must be considered in accurate modeling of the disc annulus.

Keywords Annulus fibrosus · Transversal behavior · Auxetic · Osmo-inelastic coupling · Chemo-mechanical equilibrium

1 Introduction

The intervertebral disc (IVD) is a complex fibrocartilage connecting our vertebrae from cervical part to lumbar part. This soft tissue allows body movements when our vertebral column is subjected to bend or twist. It is composed by gelatinous core, i.e., nucleus pulposus (NP), retained by adjoining concentric fiber-reinforced lamellae, i.e., annulus fibrosus (AF). As other cartilages, the IVD hydration influences the response by reaction between mobile ions in the physiological fluid and fixed charges of the extracellular matrix (ECM). The fluid is a major contributor to the IVD functionality, by varying according to external mechanical loads and internal osmotic pressure and by ensuring in vivo nutrient supply. Indeed, under mechanical loading, the fluid, flowed out, leads to chemical imbalances that generate fluid inflow [1, 2]. The time-dependent response of the disc tissues is largely governed by the interactions between the inelastic features of the tangled ECM (representing all non-fibrillar "solid" components) and the surrounding physiological fluid by osmotic effect [3–11]. The resulting chemo-mechanical couplings in the disc tissues are now well accepted but not fully understood [12, 13] and corresponding data are rare in the literature. In the particular case of the AF, some very interesting studies examined the "intrinsic" tensile response of a single lamella, regarded as the elementary

✉ Fahmi Zaïri
fahmi.zairi@polytech-lille.fr

[1] Civil Engineering and geo-Environmental Laboratory (EA 4515 LGCgE), Lille University, 59000 Lille, France

[2] ENIM, Mechanical Engineering Laboratory, Monastir University, 5019 Monastir, Tunisia

[3] Ramsay Générale de Santé, Hôpital privé Le Bois, 59000 Lille, France

structural unit of the entire annulus, in relation to regional (circumferential and radial) variation in orientation/content of collagen fibers [4, 14]. Nonetheless, considering the AF at the level of a single lamella cannot allow assessing the interactions between the "solid" components (ECM and collagen fibers), ions, and fluid. In particular, the successive lamellae of the AF exhibiting alternate fiber angles are inter-spaced by an interlamellar matrix that could have a strong implication in the inter-lamellae fluid exchanges through the layered soft tissue [10, 11]. This ground substance assuring the connection between lamellae has only been appreciated in very recent studies from structural/mechanical viewpoint [8, 12–21]. Although the IVD undergoes a multiaxial loading during body movements, the permanent compression (due to muscular tension and body weight) in the axial direction generates a NP swelling that exposes the AF to tensile stresses in the circumferential direction prior to further loading type [22]. Tension is thus an important loading mode in annulus and the investigation of the tensile response of multi-lamellae annulus tissues along with inter-lamellae interactions, from outer of the annulus towards the nucleus (radial direction), is essential for a thorough understanding of the functionality of the IVD.

In this regard, the quantitative determination of the Poisson's ratio in AF specimens, composed by multiple lamellae stretched in the circumferential direction (see Fig. 1), would allow a plausible explication of the chemo-mechanical mechanisms in the soft tissue and its related time dependency. Despite the importance of the annulus chemo-mechanical properties, corresponding data are rare in the literature. There are only the works of Baldit et al. [23], Derrouiche et al. [10], and Kandil et al. [11] which report data of this type in the plane of successive lamellae (radial direction) and their time dependency. Poisson's ratio is a two-dimensional material property describing the transversal behavior of axially stretched specimens and is between 0 and 0.5 for almost all existing materials. Dependent on the observed direction, an out-of-bonds Poisson's ratio was usually observed in the fibers plane of specimens (plane formed by axial and circumferential directions in Fig. 1) with scattered values between 0.3 and 4.64 [23–29]. In the lamellae plane (plane formed by radial and circumferential directions in Fig. 1), annulus exhibits an auxetic (negative Poisson's ratio) behavior [10, 11, 23]. The auxeticity is not common in most everyday materials, but negative values of this material property were also reported for other biological tissues such as cat skin [30], cow teat skin [31], human cancellous bone [32], bovine arteries [33], and human, pig, and sheep Achilles tendon [34]. The study of the time-dependent transversal response in the two annulus planes will improve our understanding of the disc mechanics.

In this study, full-field transversal strains are determined simultaneously in lamellae plane (LP) and in fibers plane (FP) of fresh multi-lamellae annulus specimens subjected to both quasi-static and relaxation loading. The "intrinsic" response is carefully evaluated in relation to the collagen fibers content, the osmolarity, and the strain rate. The statistical significance of the strain rate and osmolarity effects is estimated on the material properties (elastic stiffness and Poisson's ratios) in order to highlight the osmo-inelastic coupling. The two Poisson's ratios, obtained in short- and long-term experiments, are presented as indicators of the chemo-mechanical coupling in the aim to provide valuable insights into the underlying physical mechanisms.

2 Materials and methods

2.1 Specimen preparation

The disc extraction procedure and the specimen preparation are delicate. A special attention was given to the preservation of the tissue throughout the extraction procedure. Fifteen AF specimens were extracted from cervical bovine spine within 2 days after death. AF ventro-inner (VI) and ventro-outer (VO) parts were carefully separated from IVD using a surgical tool along circumferential direction. As illustrated in Fig. 1, VI and VO parts were then separated to have specimens of square cross section of

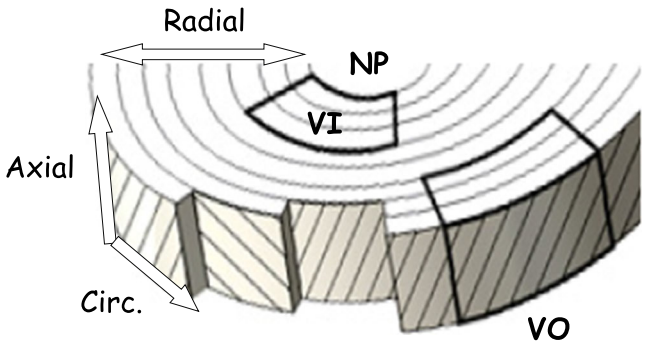

Fig. 1 Schematic view of the harvest region for multi-lamellae annulus samples of square cross section. VI, ventro-inner; VO, ventro-outer; NP, nucleus pulposus

approximately $25 \times 10 \times 10$ mm^3. The specimens had a regular geometry with flat surfaces in order to obtain accurate macro-response and local strain measurements. Bovine was selected in reason of its size, facilitating local strain measurements. After excision, AF specimens were immerged in 9 g/L saline solution during 100 min in order to re-establish hydration due to low humidity of storage room in abattoir [35]. The extracted AF specimens were stored at 4 °C at maximum 2 days before testing. Fresh specimens were used to avoid any storage effects in terms of temperature and duration. Gripping of the AF specimen is a difficult task for the mechanical tests due to the softness of the tissue and potential failure of the bone with grip pressure. In accordance with the literature, the AF specimen was glued to aluminum plates using cyanoacrylate and then mounted on the testing machine [23, 36].

2.2 Methods

The tests were carried out at room temperature on the electro-pulse mechanical machine (Instron-5500) with 1-kN load cell. Quasi-static and relaxation tests were performed under axial, i.e., circumferential in IVD, controlled displacement to characterize both the evolution in stress and the evolution in transversal strains, while the specimen is constantly immerged in a saline solution with various concentrations.

The results reported in this investigation follow the protocol illustrated in Fig. 2. Prior to each experiment, a three-step preconditioning is applied to ensure repeatability of the mechanical response. After the first step of 30 min of mechanical rest, the AF specimens were preconditioned by 10 cycles with an axial strain amplitude of 1% at a rate of 10^{-3} s^{-1} in order to stimulate chemical equilibrium and fluid transfer. Then, the specimens were carefully preloaded at 0.1 N before testing and stretched at an axial strain of 7% at a rate of 10^{-3} s^{-1}. The Mullins effect removing improves the repeatability of the response and ensures the specimen adherence with the aluminum plates.

Two kinds of experiments were performed to characterize the AF inelastic behavior in relation with the osmolarity.[1] The first one consists in a quasi-static tensile loading-unloading test at a maximum axial strain of 5% (Fig. 2a). The second one consists in a relaxation test in which the axial strain was ramped at a prescribed level and maintained constant during a holding time sufficient to reach the stabilization in load (Fig. 2b).

The strain rate sensibility was investigated by applying successively the following axial strain rates: 2×10^{-5} s^{-1}, 2×10^{-4} s^{-1}, and 2×10^{-3} s^{-1}. For each strain rate, experiments were repeated with increasing NaCl concentrations (0 g/L hypo-osmotic solution, 9 g/L iso-osmotic solution, and then 18 g/L hyper-osmotic solution) in order to highlight the osmo-inelastic coupling.

2.3 Statistical analysis

Two-way ANOVA was used to determine the effect of strain rate and NaCl concentration on elastic stiffness and Poisson's ratios. Significance was defined as $p < 0.05$. Fifteen specimens were stretched at the same strain rate and NaCl concentration, and the results were analyzed by one-way ANOVA. Standard deviation at a 95% confidence was estimated about 6.83% with a $p = 0.0084$ indicating statistical significance of the study.

2.4 Full-field strain measurements

A digital image correlation (DIC) system constituted by a charged couple device (CCD) camera (Imager E-lite) interfaced with a computer for image digitizing and analyzing (Davis software developed by Lavision) was used to calculate a two-dimensional (2D) field of in-plane displacements. The lens axis of the CCD camera was kept perpendicular to the front face of the AF specimen to capture the 2D full-field displacements in FP. The 2D full-field displacements in LP were obtained via a right-angle prism placed beside the AF specimen. A schematic overview of the experimental setup is shown in Fig. 3. DIC measurements consist in correlating the gray levels of each deformed specimen image to their counterpart of the undeformed specimen image. To obtain randomized gray level distributions, an artificial random speckle pattern was applied on both FP and LP using an airbrush filled with matt paint. It was assured that the speckles were non-overlapped and had an optimal size. A typical size between 3 and 5 pixels has been used by acting on the airbrush spraying flow and its distance from the specimen [37, 38]. The deformed specimen images were recorded at a frequency of 3 Hz with resolution of 290 pixels/mm and size of 1628×1236 pixels. The zone of interest (ZOI) of each image was divided into small square subsets of size 48×48 pixels. The in-plane displacement vector was determined in the center point of each subset. In order to optimize the ZOI size, preliminary tests were performed by comparing the applied axial strain with the local axial strain measured by the DIC. The best results were recorded

[1] The interaction between inelastic effects and osmolarity effects will be termed as osmo-inelastic coupling.

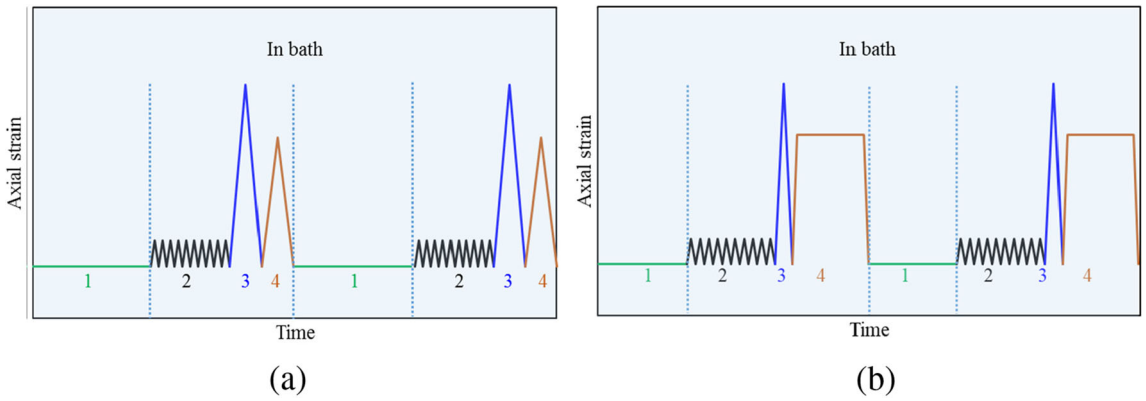

Fig. 2 Experimental design for two successive tests: (**a**) quasi-static test and (**b**) relaxation test ((1) mechanical rest, (2) successive low-strain tensions, (3) Mullins effect removing, (4) test)

for a central window at a distance of 1 mm from each edge of the specimen. Referring to these observations and literature, an inner central ZOI was considered optimal in order to avoid cyanoacrylate effect or unlikely small irregularity of the lateral edges. A root mean square error of 9.7% from the correlation process is estimated by imposing a rigid body move to AF specimen, griped at one side and free at the other one.

From the full-field strains averaged in the ZOI, the actual specimen cross section was estimated. The stress was determined as the ratio of the actual load recorded by the load cell and the actual specimen cross section. The elastic stiffness E was determined by fitting a simple neo-Hookean elastic relationship to the tensile response in terms of axial stress as a function of axial strain. Poisson's ratios ν_{LP} and ν_{FP} were calculated from the ratio between the transversal strains, in LP and in FP, respectively, and the axial strain.

3 Results

3.1 Quasi-static response

Figures 4 and 5 present typical curves of the AF stress-stretch response for the two locations in IVD, i.e., VI and VO. The effects of the microstructure, the biochemical environment, and the strain rate on the hysteretic response can be observed. The regional

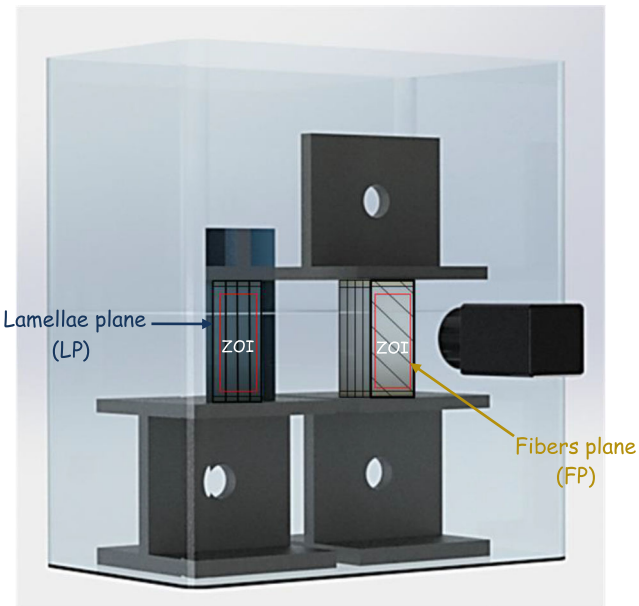

Fig. 3 Schematic view of annulus specimen with simultaneous local displacement measurements in the zone of interest (ZOI) of fibers plane (FP) and lamellae plane (LP) using a right-angle prism. The loading axis is the circumferential direction

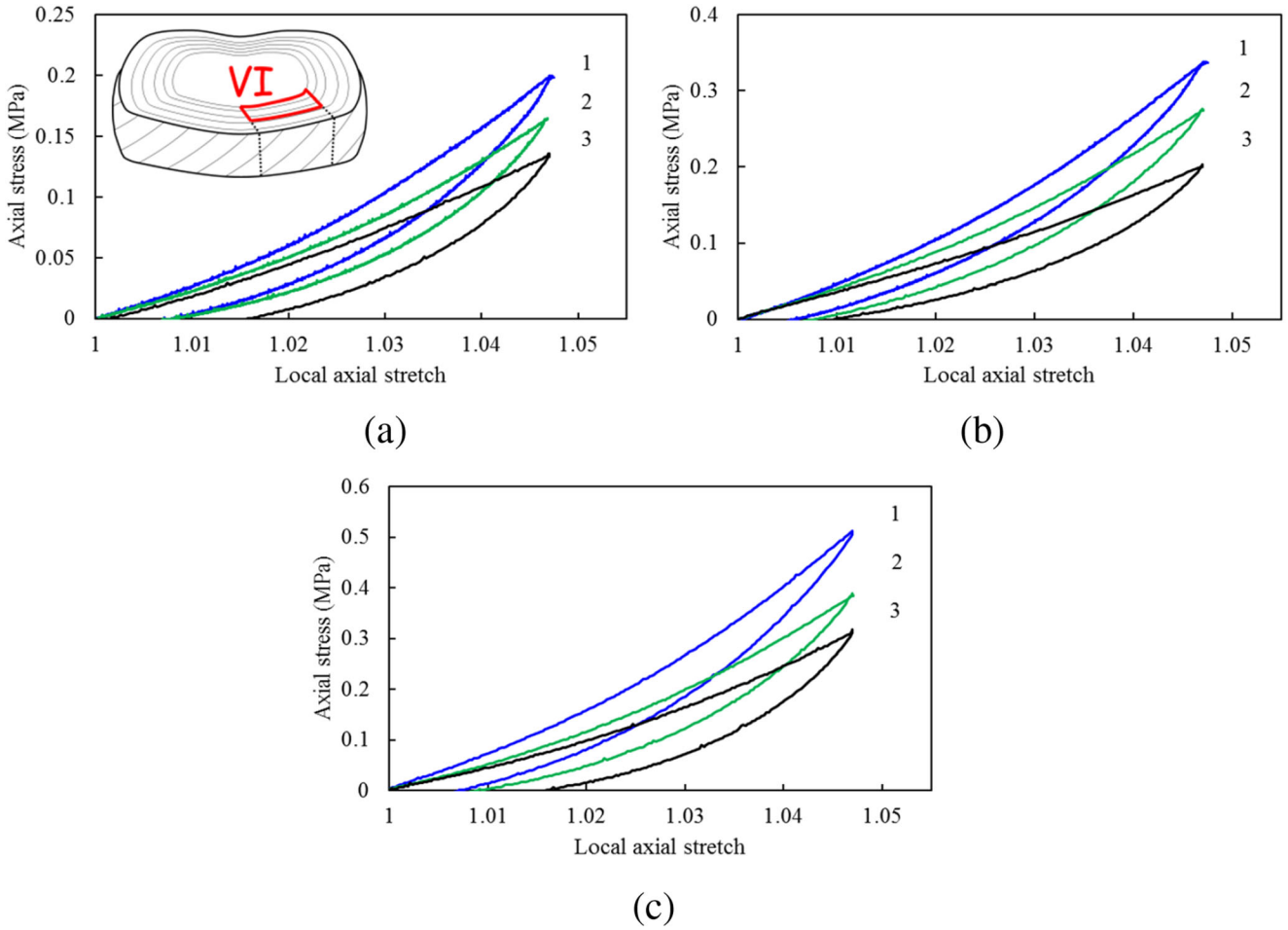

Fig. 4 Typical curves of the VI stress-stretch response at three different strain rates ((1) 2×10^{-3} s^{-1}, (2) 2×10^{-4} s^{-1}, (3) 2×10^{-5} s^{-1}) for **a** 0 g/L, **b** 9 g/L, and **c** 18 g/L NaCl concentrations

variation allows establishing the relationship between the AF mechanical response and the collagen fibers content, the amount of collagen fibers decreasing towards the nucleus. The elastic stiffness and Poisson's ratios are presented in Figs. 6 and 7 along with strain rate and osmolarity effects. Both effects are statistically significant on the elastic stiffness for VI specimen with $p = 0.05$ and $p = 0.0045$, respectively. These effects are more evidenced for the VO specimen with $p < 0.001$ for both effects. The AF tissue stiffening with the salt concentration shows the strong osmotic dependency of the mechanical response. The osmolarity dependence of the strain rate sensitivity is more pronounced in VI than in VO, suggesting that high fibers content could hide the osmotic contribution.

The transversal behavior is described by the apparent Poisson's ratios reported in Fig. 7. The term "apparent" is employed in order to point out the fluid flow dependency of this two-dimensional material property, out of the classical bounds: higher than 0.5 in FP and negative in LP. The apparent Poisson's ratio seems to reach an equilibrated value in FP when the strain rate decreases with relative osmolarity dependency in VI ($p = 0.01$ and $p < 0.001$ for strain rate and osmolarity effects, respectively). In VO, the osmolarity dependency is weak in FP and the strain rate effect is not significant ($p > 0.05$), confirming that the collagen fibers contribution is preponderant in the mechanical response. In LP, the interesting swelling presents strong variation with strain rate and osmolarity in both VO and VI ($p < 0.01$). The collagen reinforcement contribution is still evidenced with lower Poisson's ratio values in VO.

3.2 Relaxation response

Typical results of chemo-relaxation tests are presented in Fig. 8 in terms of load evolution. The load seems to evolve towards an end, if the hold time is sufficiently long, corresponding to a stabilized relaxed load. The normalized load is found markedly dependent on the strain rate (Fig. 8a). The strain level significantly affects both the maximum load and the relaxed load.

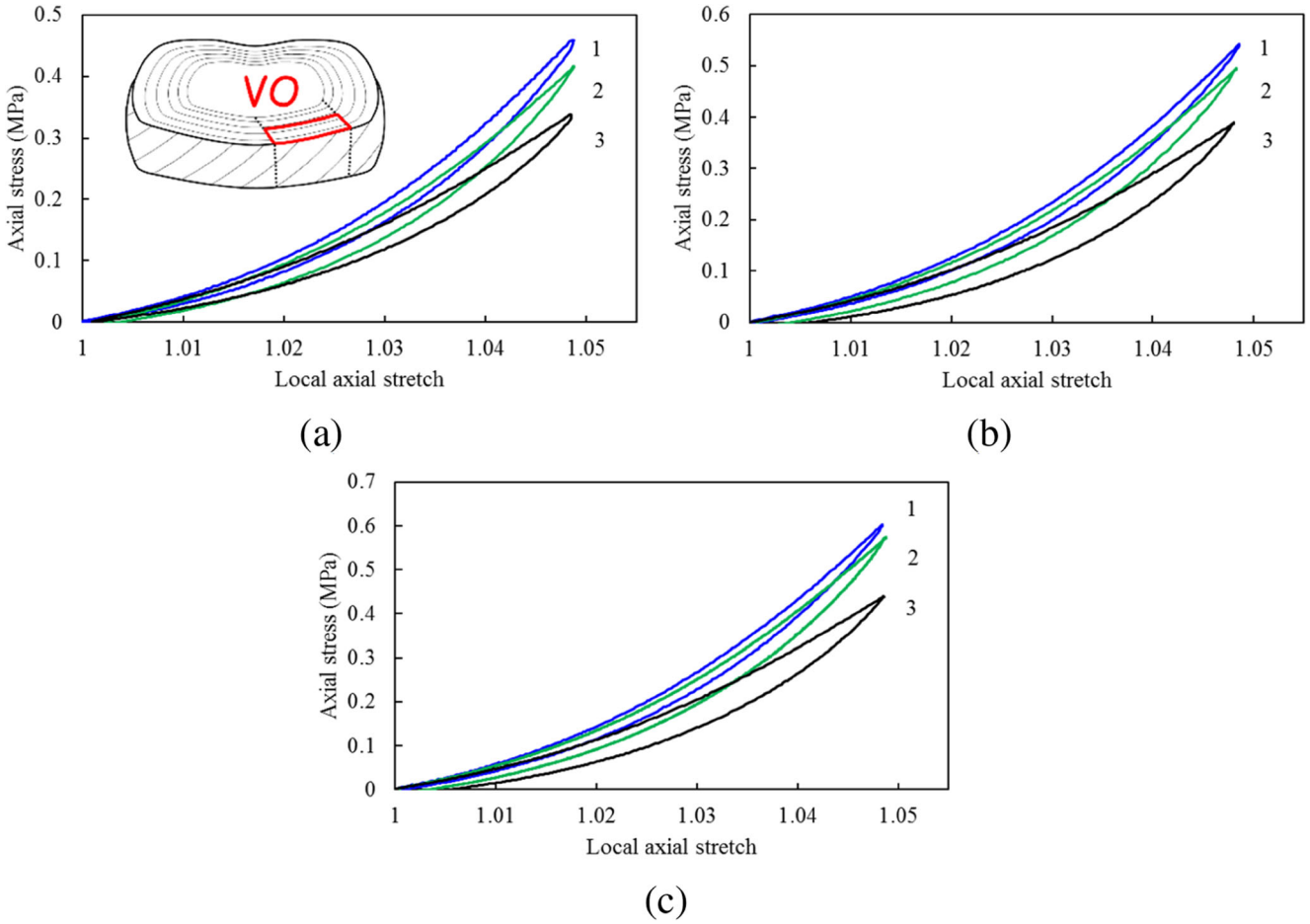

Fig. 5 Typical curves of the VO stress-stretch response at three different strain rates ((1) 2×10^{-3} s^{-1}, (2) 2×10^{-4} s^{-1}, (3) 2×10^{-5} s^{-1}) for **a** 0 g/L, **b** 9 g/L, and **c** 18 g/L NaCl concentrations

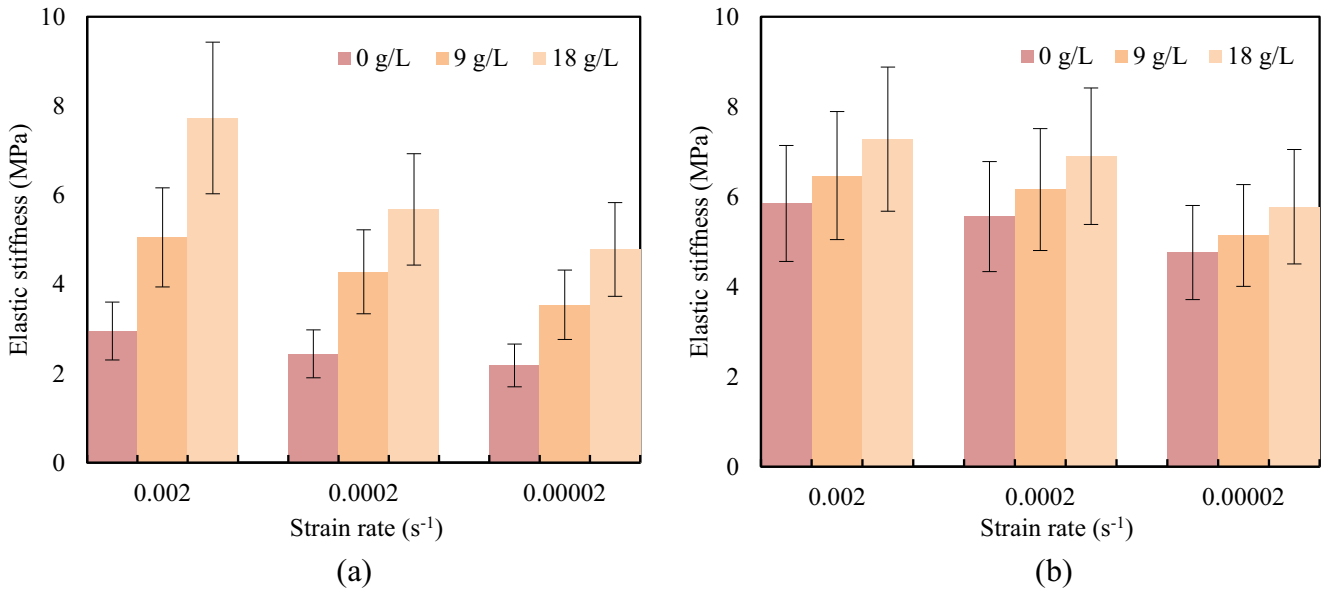

Fig. 6 Osmolarity and strain rate effects on the elastic stiffness, *E*, of two disc regions: **a** VI and **b** VO. The two factors change significantly the annulus stiffness ($p < 0.05$)

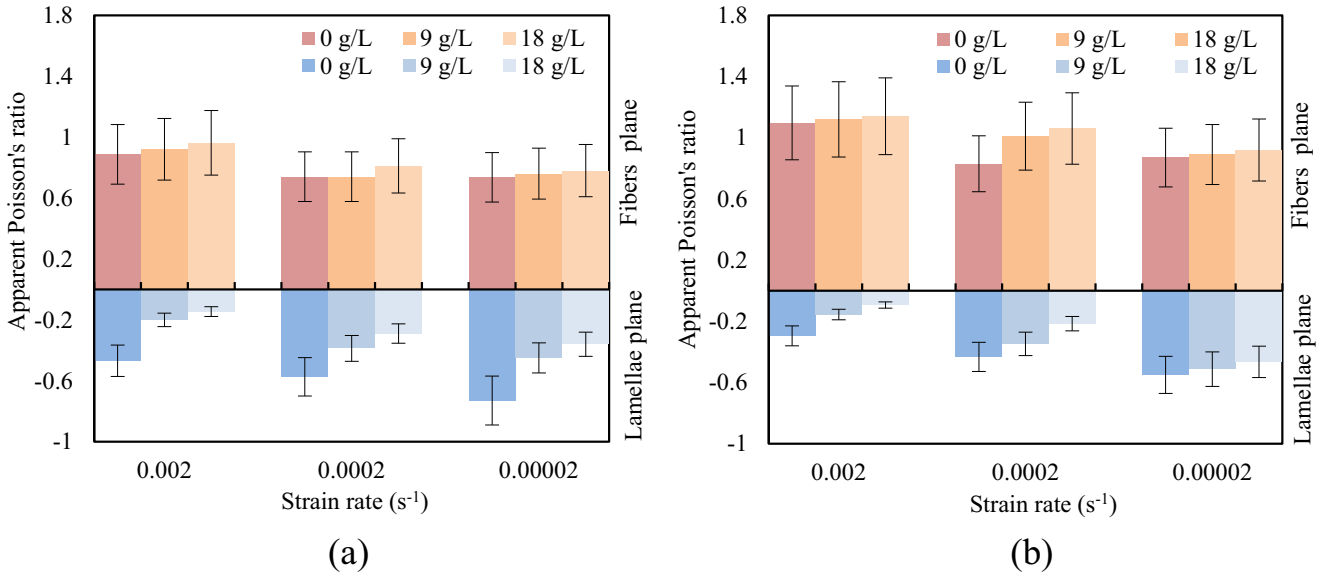

Fig. 7 Osmolarity and strain rate effects on the two apparent Poisson s ratios, ν_{FP} and ν_{LP}, of two disc regions: **a** VI and **b** VO. The two factors change significantly the annulus transversal behavior in lamellae plane ($p < 0.05$)

Nevertheless, the normalized load is found independent on the strain level (Fig. 8b), suggesting a proportional effect of the applied stretch on the fluid exchange. The external solution concentration has a strong effect on the chemo-relaxation response of the AF tissue (Fig. 8c). By favoring the fluid transfer, the osmolarity has for effect to increase the AF stiffness at the macro-scale

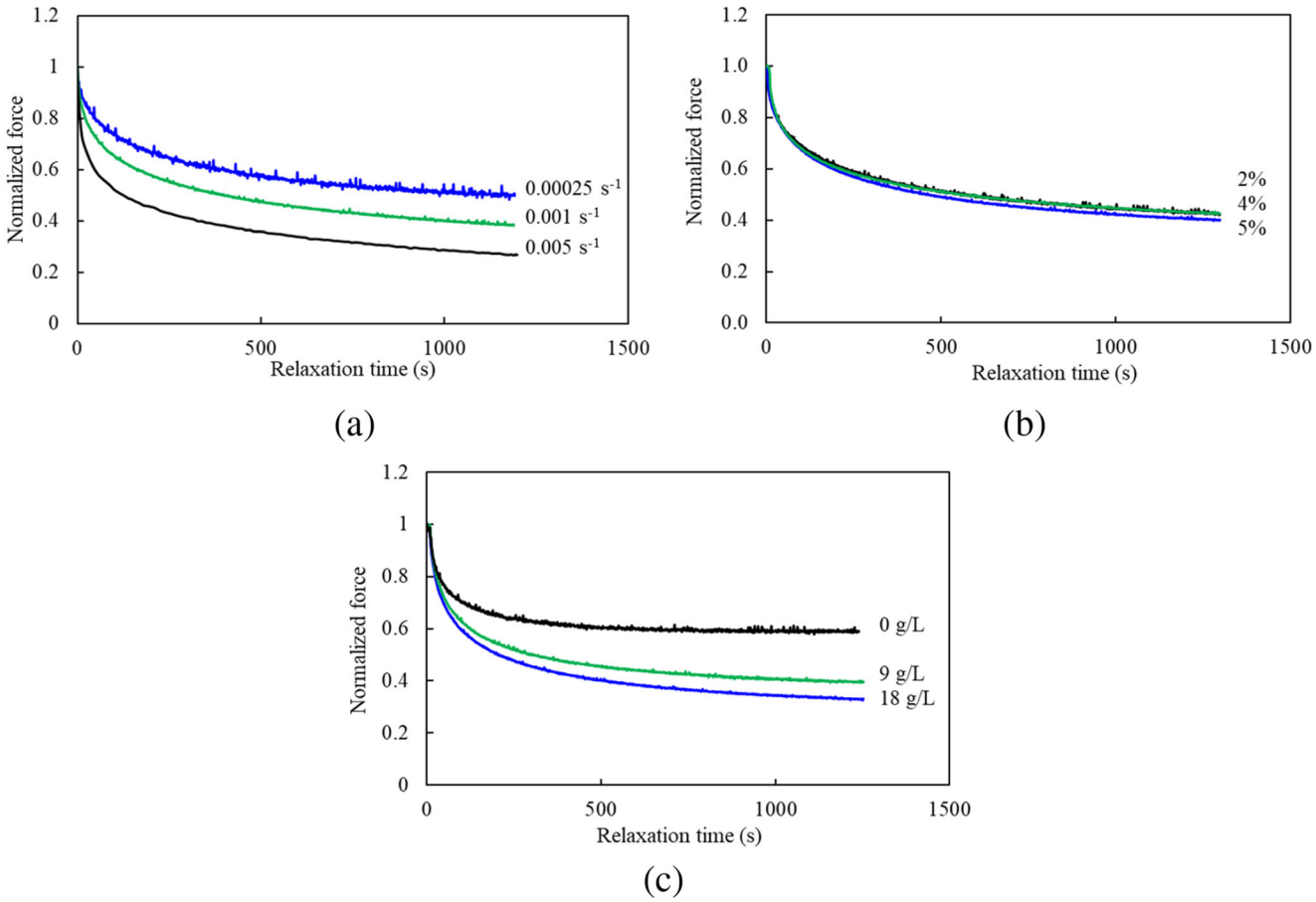

Fig. 8 Typical load evolution under relaxation with **a** strain rate, **b** strain level, and **c** osmolarity effects

and the local stresses. The equilibrium response clearly depends on the environment. With higher local stresses previous to the relaxation, the chemical imbalances are higher and the relaxed load becomes lower with more fluid exchange.

The transversal behavior can provide some additional insights into the structural changes during the chemo-relaxation. A typical result is provided in Fig. 9a. As a consequence of the applied axial stretching, the LP and FP transversal strains increase. The transversal strains represent structural changes due to fluid content evolution. In FP, the tightening reaches about a 3% transversal strain for a 3.5% axial strain. In the meantime, the AF swells at about a 1.5% transversal strain in LP. More interestingly, during the relaxation period, an opposite evolution is observed for both transversal strains until to reach a stabilized value due to the chemo-mechanical equilibrium. The equilibrium transversal strain is equal to about 1.7% in FP and close to zero in LP.

Apparent Poisson's ratio may be considered as an indicator of the AF local response in relation with internal changes. As a consequence of the opposite evolution in transversal strains between stretching and relaxation, the apparent Poisson's ratios change during the chemo-relaxation process as shown in Fig. 9b. The apparent Poisson's ratio decreases in FP and increases in LP, to reach stabilized values in a more classical range, about 0.5 in FP and 0.02 in LP. The LP auxetic response vanishes after stabilization. The osmo-inelastic effects on the relaxed value of Poisson's ratio are given in Fig. 10. The relaxed value is nearly not affected by the strain rate but the increase in osmolarity leads to decrease the relaxed value in FP and to increase it in LP ($p < 0.05$).

4 Discussion

Our experimental observations provide valuable insights into the chemo-mechanical coupling and the origin of the time dependency. The underlying mechanisms involve both ECM rearrangement and ionic transfer by fluid exchange. We evidence that the AF tissue exhibits different transversal behaviors in its two planes, namely FP and LP. An antagonist variation is found during relaxation, suggesting a fluid exchange between FP and LP. The apparent Poisson's ratio is taken as indicator of the chemo-mechanical coupling in the aim to better understand the capability of the AF tissue to maintain its internal chemical balance under external mechanical loading.

Under a quasi-static loading, the volume variation, due to Poisson's ratio effect, is found regional-dependent and higher in VI than in VO. The collagen network seems to cause this difference, since its contribution avoids internal changes. The volume variation is a function of ionic content in solution to equilibrate chemical and mechanical parts of the response. Indeed, the volume variation decreases with NaCl concentration. This phenomenon may be explained by the fact that in a hyper-osmotic environment, AF needs to swell lesser to catch mobile ions in solution. The hyper-osmotic effect is also responsible of a microstructure tightening inducing a smaller fluid volume in the tissue. If the environment becomes hypo-osmotic, the AF swelling is higher in order to catch more ions and to reach the chemo-mechanical equilibrium. This time dependency of the chemo-mechanical response is caused by the fluid transfer between FP and LP. The mechanical stress during the stretching contributes to the fluid flow inducing a chemical stress which

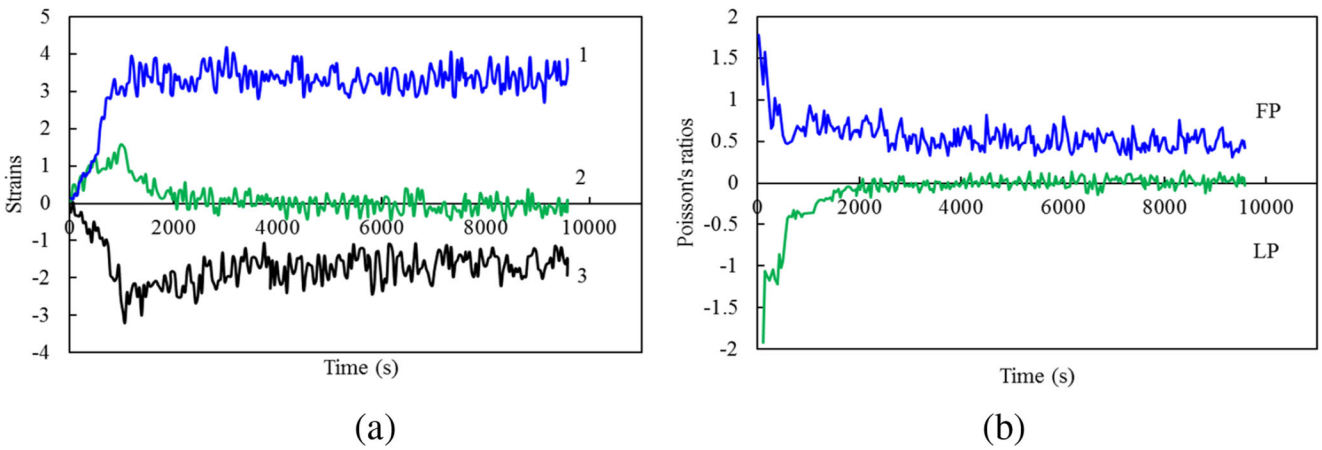

Fig. 9 Typical evolution under relaxation of **a** local strains (in %) ((1) axial strain, (2) LP transversal strain, (3) FP transversal strain) and **b** the two apparent Poisson's ratios, ν_{FP} and ν_{LP}

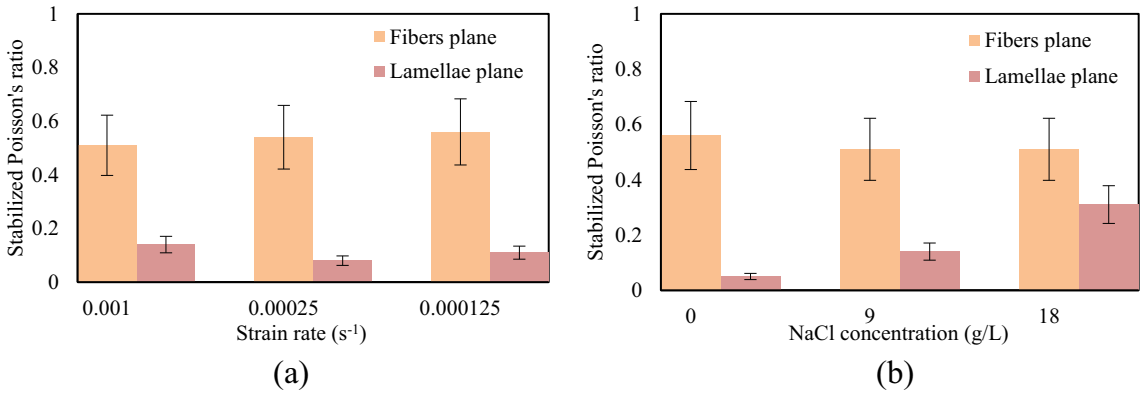

Fig. 10 Stabilized Poisson's ratio, ν_{FP} and ν_{LP}, of VI with **a** strain rate and **b** osmolarity effects. Similar results are obtained for different strain rates ($p > 0.05$) but the osmolarity affects the annulus transversal behavior in the two planes ($p < 0.05$)

provokes the fluid recovering during the relaxation until equilibrium, in which chemical and mechanical stresses become equilibrated. The transferred fluid content increases with the increase in strain level. Indeed, the chemical unbalance is directly related to the fluid exchange. By increasing the prescribed axial strain, at a given strain rate, a higher ionic content in the tissue is required to reach the chemo-mechanical equilibrium and the observable relaxed state at the macro-scale.

The osmo-relaxation in AF tissue is a reversible process dependent on fluid exchange. Other reversible factors may participate to the stress relaxation in the AF tissue such as the ECM rearrangement [39]. The stabilized relaxed load is reached more rapidly at a zero NaCl concentration since a limiting fluid transfer is involved. Higher NaCl concentrations act on the fluid transfer inside the tissue. As a consequence, the degree, to which the AF tissue is relaxed, increases with the osmolarity. The hold time needed to reach the stabilized relaxed load increases with the osmolarity. The equilibrium response clearly depends on the environment since proteoglycan macromolecules become closer under hyper-osmotic environment in order to reduce the fluid content and to establish the chemical equilibrium. The microstructure state may be then affected by the chemical stress created with increase in mobile ionic components. The chemo-induced micro-structure rearrangement is then responsible for local mechanical stresses that induce more fluid flowed out. With higher local stresses previous to the relaxation, the chemical imbalances are higher and the relaxed load becomes lower with more fluid exchange.

Fluid transfer inside the tissue is an explanation of the chemo-relaxation response of the AF during the maintaining of the axial stretch. The quantity of flowed fluid is dependent on the rate at which the maintained axial stretch is reached. Indeed, the fluid flow is more important when the strain rate increases. During the stretching, the local strains or stresses are heterogeneous and dependent on the applied strain rate. The higher the strain rate is, the higher the local stresses are. At high strain rate, the highly localized stresses favor the fluid transfer towards zones with lesser stresses. The fluid content in the tissue decreases with the intensity of the local stresses and with the strain rate. The relaxation response is then dependent on the fluid exchange during the previous stretching rate. Since a higher amount of fluid is transferred due to local stresses during the initial stretching when the strain rate increases, the chemical unbalance is higher. Therefore, during the relaxation, a higher transferred fluid content is necessary to reach the chemo-mechanical equilibrium of the tissue. That leads to the observable increase of the relaxation rate at the macro-scale.

The swelling in LP and the tightening in FP suggest a transfer mechanism between the two planes during the relaxation. Lower local stresses in LP may explain the fluid transport towards this plane and the chemical stresses induce the partial return of a fluid content. Figure 11 gives our interpretation in the form of a schematic view. Fluid flow out creates ionic imbalance and chemical stress. The mechanical strains/stresses are higher in FP and water flows out towards ground substance in which the stress state is lower. The tightening in FP due to flow out and the swelling in LP is observed due to this difference in local mechanical stresses. The difference in chemical state forces a part of fluid to come back to its equilibrium state and apparent Poisson's ratios to reach usual bounds. In equilibrium, the osmotic pressure is equilibrated by the mechanical state [40].

The new information of this study can help to design disc prostheses to better mimic the function of the healthy disc on what our research group is currently engaged [41, 42]. Additionally, the present data provide direct input for microstructure-based chemo-mechanical constitutive models of the annulus osmo-inelastic response [10, 11]. They are crucial prerequisite for meaningful finite element models of the healthy disc by providing accurate predictions of the chemo-mechanical response.

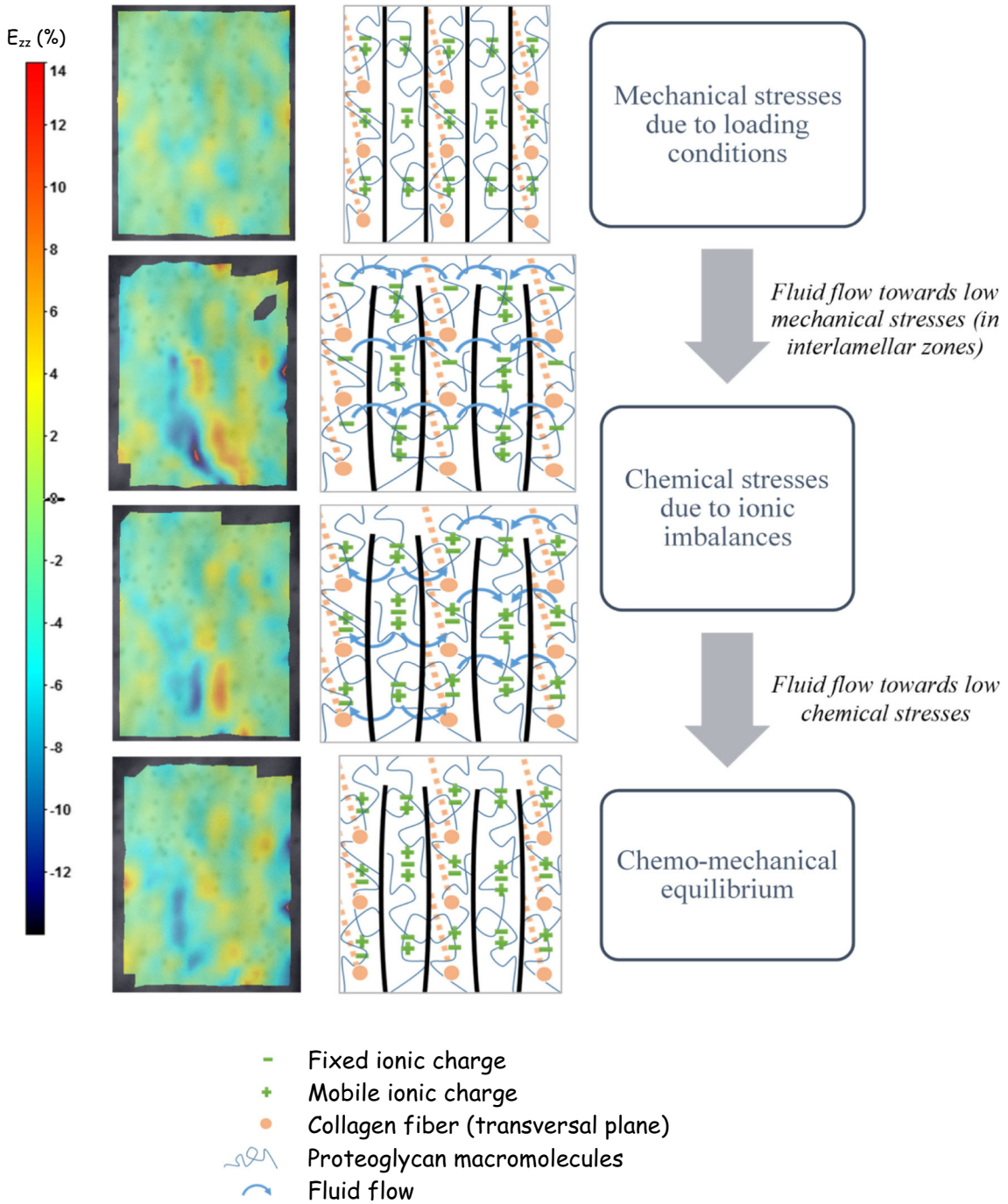

Fig. 11 Chemo-mechanical mechanisms in lamellae plane. The mapping pictures correspond to the transversal strain in lamellae plane for different loading steps

5 Conclusions

In this study, the transversal response of the annulus is determined in order to bring a better understanding of the disc functionality involving auxeticity, inelasticity, and osmolarity effects. The time dependency and chemical dependency of the auxetic behavior in lamellae plane highlight the osmo-inelastic coupling. Although the present study is based on a relatively small number of specimens, it is the first observation of the establishment of chemo-mechanical equilibrium. The equilibrium altered by osmolarity is a process involving local changes in fluid content until a balance between chemical and mechanical states.

Further works are needed to validate the observed features to human annulus especially in relation with aging and degeneration.

References

1. Drost, M.R., Willems, P., Snijders, H., Huyghe, J.M., Janssen, J.D., Huson, A.: Confined compression of canine annulus fibrosus under chemical and mechanical loading. J. Biomech. Eng. **117**, 390–396 (1995)
2. Schmidt, H., Reitmaier, S., Graichen, F., Shirazi-Adl, A.: Review of the fluid flow within intervertebral discs - how could in vitro measurements replicate in vivo? J. Biomech. **49**, 3133–3146 (2016)
3. Race, A., Broom, N.D., Robertson, P.: Effect of loading rate and hydration on the mechanical properties of the disc. Spine. **25**, 662–669 (2000)
4. Holzapfel, G.A., Schulze-Bauer, C.A.J., Feigl, G., Regitnig, P.: Single lamellar mechanics of the human lumbar anulus fibrosus. Biomech. Model. Mechanobiol. **3**, 125–140 (2005)
5. Kemper, A.R., McNally, C., Duma, S.M.: The influence of strain rate on the compressive stiffness properties of human lumbar intervertebral discs. Biomed. Sci. Instrum. **43**, 176–181 (2007)
6. Newell, N., Grigoriadis, G., Christou, A., Carpanen, D., Masouros, S.D.: Material properties of bovine intervertebral discs across strain rates. J. Mech. Behav. Biomed. Mater. **65**, 824–830 (2016)
7. Newell, N., Little, J.P., Christou, A., Adams, M.A., Adam, C.J., Masouros, S.D.: Biomechanics of the human intervertebral disc: a review of testing techniques and results. J. Mech. Behav. Biomed. Mater. **69**, 420–434 (2017)
8. Tavakoli, J., Costi, J.J.: New findings confirm the viscoelastic behaviour of the inter-lamellar matrix of the disc annulus fibrosus in radial and circumferential directions of loading. Acta Biomater. **71**, 411–419 (2018)
9. Derrouiche, A., Zaouali, A., Zaïri, F., Ismail, J., Chaabane, M., Qu, Z., Zaïri, F.: Osmo-inelastic response of the intervertebral disc. Proceedings of the Institution of Mechanical Engineers. Part H. J. Eng. Med. **233**, 332–341 (2019)
10. Derrouiche, A., Zaïri, F., Zaïri, F.: A chemo-mechanical model for osmo-inelastic effects in the annulus fibrosus. Biomech. Model. Mechanobiol. **18**, 1773–1790 (2019)
11. Kandil, K., Zaïri, F., Derrouiche, A., Messager, T., Zaïri, F.: Interlamellar-induced time-dependent response of intervertebral disc annulus: a microstructure-based chemo-viscoelastic model. Acta Biomater. **100**, 75–91 (2019)
12. Emanuel, K.S., van der Veen, A.J., Rustenburg, C.M.E., Smit, T.H., Kingma, I.: Osmosis and viscoelasticity both contribute to time-dependent behaviour of the intervertebral disc under compressive load: a caprine in vitro study. J. Biomech. **70**, 10–15 (2018)
13. Vergroesen, P.P.A., Emanuel, K.S., Peeters, M., Kingma, I.: Are axial intervertebral disc biomechanics determined by osmosis? J. Biomech. **70**, 4–9 (2018)
14. Ebara, S., Iatridis, J.C., Setton, L.A., Foster, R.J., Mow, V.C., Weidenbaum, M.: Tensile properties of nondegenerate human lumbar anulus fibrosus. Spine. **21**, 452–461 (1996)
15. Pezowicz, C.A., Robertson, P.A., Broom, N.D.: The structural basis of interlamellar cohesion in the intervertebral disc wall. J. Anat. **208**, 317–330 (2006)
16. Michalek, A.J., Buckley, M.R., Bonassar, L.J., Cohen, I., Iatridis, J.C.: Measurement of local strains in intervertebral disc anulus fibrosus tissue under dynamic shear: contributions of matrix fiber orientation and elastin content. J. Biomech. **42**, 2279–2285 (2009)
17. Adam, C., Rouch, P., Skalli, W.: Inter-lamellar shear resistance confers compressive stiffness in the intervertebral disc: an image-based modelling study on the bovine caudal disc. J. Biomech. **48**, 4303–4308 (2015)
18. Mengoni, M., Luxmoore, B.J., Wijayathunga, V.N., Jones, A.C., Broom, N.D., Wilcox, R.K.: Derivation of inter-lamellar behaviour of the intervertebral disc annulus. J. Mech. Behav. Biomed. Mater. **48**, 164–172 (2015)
19. Vergari, C., Mansfield, J., Meakin, J.R., Winlove, P.C.: Lamellar and fibre bundle mechanics of the annulus fibrosus in bovine intervertebral disc. Acta Biomater. **37**, 14–20 (2016)
20. Tavakoli, J., Elliott, D.M., Costi, J.J.: Structure and mechanical function of the inter-lamellar matrix of the annulus fibrosus in the disc. J. Orthop. Res. **34**, 1307–1315 (2016)
21. Tavakoli, J., Elliott, D.M., Costi, J.J.: The ultra-structural organization of the elastic network in the intra- and inter-lamellar matrix of the intervertebral disc. Acta Biomater. **58**, 269–277 (2017)
22. Nachemson, A., Morris, J.M.: In vivo measurements of intradiscal pressure: discometry, a method for the determination of pressure in the lower lumbar discs. J. Bone Joint Surg. **46**, 1077–1092 (1964)
23. Baldit, A., Ambard, D., Cherblanc, F., Royer, P.: Experimental analysis of the transverse mechanical behaviour of annulus fibrosus tissue. Biomech. Model. Mechanobiol. **13**, 643–652 (2014)
24. Elliott, D.M., Setton, L.A.: Anisotropic and inhomogeneous tensile behavior of the human annulus fibrosus: experimental measurement and material model predictions. J. Biomech. Eng. **123**, 256–263 (2001)
25. Guerin, H.A.L., Elliott, D.M.: Degeneration affects the fiber reorientation of human annulus fibrosus under tensile load. J. Biomech. **39**, 1410–1418 (2006)
26. Lewis, N.T., Hussain, M.A., Mao, J.J.: Investigation of nano-mechanical properties of annulus fibrosus using atomic force microscopy. Micron. **39**, 1008–1019 (2008)
27. O'Connell, G.D., Guerin, H.L., Elliott, D.M.: Theoretical and uniaxial experimental evaluation of human annulus fibrosus degeneration. J. Biomech. Eng. **131**, 1–7 (2009)
28. O'Connell, G.D., Sen, S., Elliott, D.M.: Human annulus fibrosus material properties from biaxial testing and constitutive modeling are altered with degeneration. Biomech. Model. Mechanobiol. **11**, 493–503 (2012)
29. Singha, K., Singha, M.: Biomechanism profile of intervertebral disc's (IVD): strategies to successful tissue engineering for spinal healing by reinforced composite structure. J. Tissue Sci. Eng. **3**, 1000118 (2012)

30. Veronda, D.R., Westmann, R.A.: Mechanical characterization of skin-finite deformations. J. Biomech. **3**, 111–124 (1970)
31. Lees, C., Vincent, J.F., Hillerton, J.E.: Poisson's ratio in skin. Biomed. Mater. Eng. **1**, 19–23 (1991)
32. Williams, J.L., Lewis, J.L.: Properties and an anisotropic model of cancellous bone from the proximal tibial epiphysis. J. Biomech. Eng. **104**, 50–56 (1982)
33. Timmins, L.H., Wu, Q., Yeh, A.T., Moore, J.E., Greenwald, S.E.: Structural inhomogeneity and fiber orientation in the inner arterial media. Am. J. Physiol. Heart Circ. Physiol. **298**, 1537–1545 (2010)
34. Gatt, R., Wood, M.V., Gatt, A., Zarb, F., Formosa, C., Azzopardi, K.M., Casha, A., Agius, T.P., Schembri-Wismayer, P., Attard, L., Chockalingam, N., Grima, J.N.: Negative Poisson's ratios in tendons: an unexpected mechanical response. Acta Biomater. **24**, 201–208 (2015)
35. Costi, J.J., Hearn, T.C., Fazzalari, N.L.: The effect of hydration on the stiffness of intervertebral discs in an ovine model. Clin. Biomech. **17**, 446–455 (2002)
36. Bruehlmann, S.B., Hulme, P.A., Duncan, N.A.: In situ intercellular mechanics of the bovine outer annulus fibrosus subjected to biaxial strains. J. Biomech. **37**, 223–231 (2004)
37. Zhou, P., Goodson, K.E.: Subpixel displacement and deformation gradient measurement using digital image/speckle correlation. Opt. Eng. **40**, 1613–1620 (2001)
38. Palanca, M., Tozzi, G., Cristofolini, L.: The use of digital image correlation in the biomechanical area: a review. International Biomechanics. **3**, 1–21 (2015)
39. Sverdlik, A., Lanir, Y.: Time-dependent mechanical behavior of sheep digital tendons, including the effects of preconditioning. J. Biomech. Eng. **124**, 78–84 (2002)
40. Maroudas, A.: Balance between swelling pressure and collagen tension in normal and degenerate cartilage. Nature. **260**, 808–809 (1976)
41. Jiang, Q., Zaïri, F., Frederix, C., Yan, Z., Derrouiche, A., Qu, Z., Liu, X., Zaïri, F.: Biomechanical response of a novel intervertebral disc prosthesis using functionally graded polymers: a finite element study. J. Mech. Behav. Biomed. Mater. **94**, 288–297 (2019)
42. Jiang, Q., Zaïri, F., Frederix, C., Derrouiche, A., Yan, Z., Qu, Z., Liu, X., Zaïri, F.: Crystallinity dependency of the time-dependent mechanical response of polyethylene: application in total disc replacement. J. Mater. Sci. Mater. Med. **30**, 46 (2019)

Publisher's note